Check for updates

Effect of the coexistence of albumin and H_2O_2 on the corrosion of biomedical cobalt alloys in physiological saline†

Weichen Xu,[acde] Binbin Zhang, [iD] [acd] Lihui Yang,[acd] Qiancheng Ni,[ac] Yantao Li[acd] and Fei Yu [iD] *[b]

The corrosion of Co–28Cr–6Mo and Co–35Ni–20Cr–10Mo, as biomedical alloys, has been investigated for effects of typical species (albumin and H_2O_2) in physiological saline, with their coexistence explored for the first time. Electrochemical and long term immersion tests were carried out. It was found that Co alloys were not sensitive to the presence of albumin alone, which slightly promoted anodic dissolution of Co–35Ni–20Cr–10Mo without noticeably affecting Co–28Cr–6Mo and facilitated oxide film dissolution on both alloys. H_2O_2 led to a clear drop in corrosion resistance, favouring metal release and surface oxide formation and inducing much thicker but less compact oxide films for both alloys. The coexistence of both species resulted in the worst corrosion resistance and most metal release, while the amount and composition of surface oxide remained at a similar level as in the absence of both. The effect of H_2O_2 inducing low compactness of surface oxides should prevail on deciding the poor corrosion protection ability of passive film, while albumin simultaneously promoted dissolution or inhibited formation of oxides due to H_2O_2. Corrosion resistance was consistently lower for Co–35Ni–20Cr–10Mo under each condition, the only alloy where the synergistic effect of both species was clearly demonstrated. This work suggests that the complexity of the environment must be considered for corrosion resistance evaluation of biomedical alloys.

1. Introduction

Co-based, titanium and stainless steel alloys have all been applied as materials for metallic orthopedic implants due to their high corrosion resistance and excellent biocompatibility. Their application has continuously increased and it has been estimated that the number of joint replacements will exceed 572 000 by 2030.[1] However, despite the satisfactory overall performance of these biomedical alloys, the passive films on the surface of these alloys are actually dynamic and responsive to body fluid

[a]Key Laboratory of Marine Environmental Corrosion and Bio-fouling, Institute of Oceanology, Chinese Academy of Sciences, Qingdao 266071, People's Republic of China

[b]Institute for Translation Medicine, Medical College, Qingdao University, Qingdao 266021, People's Republic of China. E-mail: feiyu@qdu.edu.cn

[c]Open Studio for Marine Corrosion and Protection, Pilot National Laboratory for Marine Science and Technology, Qingdao 266237, People's Republic of China

[d]Center for Ocean Mega-Science, Chinese Academy of Sciences, Qingdao 266071, People's Republic of China

[e]Research Development Center of Marine Science and Technology, Institute of Oceanology, Chinese Academy of Sciences, Nantong 226019, People's Republic of China

† Electronic supplementary information (ESI) available: Table 1 providing LOD and LOQ for ICP-MS measurements, Table 2 providing concentration data of ICP-MS measurement, Fig. 1–3 presenting SEM images and EDX results of the surface of Co alloy discs. See DOI: 10.1039/c9ra05699h

environment,[2] so corrosion issues have attracted great attention, as they affect the integrity of implants and lead to release of hazardous metallic ions into body fluids.[3–7] Since corrosion inevitably takes place on metals implanted in human body, the corrosion characteristics of these alloys have been studied in simulated peri-implant environments containing inorganic species (*e.g.* H_2O_2) or organic species (*e.g.* protein).[5] Specifically, the joint effect of both inorganic and organic species has been recently reported on Ti,[8,9] Zr[10] and stainless steel,[11] but the corrosion mechanisms varied with different materials.

Co-based alloys have been used successfully since the early 1970s[12,13] and are widely employed as dental devices, joint replacements, cardiovascular stents, *etc.*,[2,14–16] so material degradation resulting from corrosion has become a potential concern.[3,4,17,18] Furthermore, the concentrations of Co and Cr ions released due to corrosion have been reported to increase significantly in patients after implant surgery[19] and can be toxic at certain levels,[20] reacting with DNA, receptors, proteins and reactive oxygen species (ROS) and altering the biological environment.[5,12] In this study, H_2O_2 and albumin have been selected as typical inorganic and organic species for the purpose of corrosion resistance evaluation for biomedical Co alloys and the joint effect of both species will be discussed for the first time. This work is worth being carried out for material reliability evaluation and systematic comparison with other biomedical alloys.

Protein is a very important complex organic compound in human fluids and is regarded as the first component to interact with biomedical alloys after implantation surgeries,[21] as it adsorbs on the surface of implants.[22] However, protein adsorption is complicated when the substrate, concentration or chemical composition is considered,[23–27] as these affect the corrosion characteristics of alloys. Albumin is the most abundant protein in serum;[28] it is generally accepted that albumin is negatively charged and tends to be adsorbed on anodically dissolving metal surfaces (*i.e.* anodically charged).[29] It was found that the corrosion products of Co alloys were mainly organometallic complexes which formed at the metal/solution interface or in the solution depending on different elements in the alloys.[30] Based on previous studies, increased weight loss and ion release after the addition of albumin into physiological saline or PBS indicated accelerated corrosion rates,[11,24,31] while electrochemical impedance spectroscopy measurements showed a decrease in corrosion resistance at low concentration and an increase at high concentration.[29] An interpretation of this difference has not been given. The metal ions interact with albumin to form complexes, which may either be dissolved in the solution or precipitated on the metal surface.[24] It was also found that albumin may result in the dissolution of surface oxides, leading to the thinning of passive film.[11,31] In addition, the affinity of albumin for different elements varies, which may account for inconsistency between actual ion release and stoichiometry.[32] However, suppression of corrosion by albumin has also been reported in the literature, *e.g.* decreased corrosion rate[33] and Cr release[28] or enhanced passive film stability.[29,34] Therefore, the effect of albumin on the corrosion of biomedical alloys has not yet been fully clarified.

After implantation, immune reactions may cause inflammation and the inflammatory cells tend to attach to the implant surface[35] and release reactive oxygen species (ROS) to attack any foreign substances,[36–39] as proved by a study of CoCrMo alloy immersed in inflammatory cell culture medium.[40] H_2O_2 is a very important ROS used to simulate the inflammation process for *in vitro* studies and the extracellular H_2O_2 concentration range was found to be in the range of μM–mM.[41,42] It has been found in different alloys that H_2O_2 can facilitate the formation of oxides[11,43] or hydroxyl oxide[11] and positively shift corrosion potential.[2,11] However, corrosion resistance is reported to decrease in the presence of different concentrations of H_2O_2.[11,44–46] H_2O_2 is often regarded as a complicated species, determining both the anodic and cathodic electrochemical responses of Co alloys,[12] though its effect has not been fully clarified. It has also been suggested that ICIC (inflammatory cell-induced corrosion) of Co alloys may be self-sustaining and even a tiny amount of metallic ion release from the alloys may further aggravate inflammation.[12,47,48] In addition, corrosion products induced by Fenton reactions (H_2O_2 as a reactant) may also make a solution more oxidizing.[48,49]

The current knowledge of Co alloy corrosion in human body fluid is limited to the effects of organic species (*e.g.* albumin) alone[31,34] and inorganic species (*e.g.* H_2O_2) alone.[2,45] Hedberg[50] considered H_2O_2 and albumin in a recent study, but still separately. A much more realistic and typical condition, *i.e.* the

combination of both species, is still yet to be investigated. For the first time, this article describes an investigation on corrosion characteristics of Co alloys, including Co–28Cr–6Mo and Co–35Ni–20Cr–10Mo (also known as MP35N alloy), in the presence of both H_2O_2 and albumin. Although MP35N alloy contains a high level of Ni, the release of Ni was not reported to be severe in simulated human fluids.[51] It has also been used widely,[14,15] so the two types of alloys are compared in this work. Electrochemical and 4 month immersion tests were carried out, using polarisation curves, electrochemical impedance spectroscopy (EIS), inductively coupled plasma mass spectrometry (ICP-MS), X-ray photoelectron spectroscopy (XPS) and atomic force microscopy (AFM) techniques.

2. Material and methods

2.1. Alloy samples and solutions

Two kinds of Co alloys were used in this work: Co–28Cr–6Mo and Co–35Ni–20Cr–10Mo, both provided by the National Engineering Research Center of Advanced Steel Technology (China). Co–28Cr–6Mo and Co–35Ni–20Cr–10Mo alloys are commercially available as bars and the standards are ASTM 1537 (alloy 2 UNS R31538) and ASTM F562 (UNS R30035), respectively. The bars were cut into discs (surface area 1 cm², thickness 5 mm). Tables 1 and 2 show the chemical compositions of both alloys. The discs were soldered to electric wire, mounted in epoxy resin with 1 cm² surface area exposed for electrochemical experiments, and then successively ground with 240, 600 and 1000 grit emery paper (Riken Corundum Co., Ltd., Japan). A similar grinding procedure was applied to discs used for long term immersion tests, where both sides and the edge surface were all ground and mounting was not needed. To carry out ICP-MS tests after immersion, the discs for immersion tests were ultrasonically washed with acetone, methanol and sterilised ultra-pure water (provided by Nanjing JianCheng Technology Co., Ltd., China, resistivity no less than 18 MΩ cm) successively for 10 min each before immersion.

The solutions used in this work were physiological saline (0.9 wt% NaCl, Sinopharm Chemical Reagent Co., Ltd.) with or without the addition of 0.1 wt% bovine serum albumin (96 wt%, Shanghai Macklin Biochemical Co., Ltd.) or 1 mM H_2O_2 (30 wt% H_2O_2, Shanghai Macklin Biochemical Co., Ltd.). For convenience, they are described as PS, PS + albumin, PS + H_2O_2 and PS + albumin + H_2O_2 in the following sections. Double-distilled water and sterilised ultra-pure water were used for the electrochemical and long-term immersion tests, respectively. The test solutions were kept at 37 °C with a water bath (DF-101S, Shanghai Yuhua Co., Ltd.) or an incubator chamber (DHP-9052, Shanghai Yiheng Co., Ltd.) for the electrochemical and long-term immersion tests, respectively. The fluctuation of the controlled temperature was

Table 1 The chemical composition of Co–28Cr–6Mo alloy

Element	Cr	Mo	Mn	Fe	Ni	C	Si	Co
wt%	27.99	6.14	0.47	0.33	0.004	0.21	0.67	Balance

Table 2 The chemical composition of Co−35Ni−20Cr−10Mo alloy

Element	Ni	Cr	Mo	Mn	Fe	Ti	C	Si	Co
wt%	34.21	20.38	9.85	0.13	0.90	0.87	0.02	0.13	Balance

within ±1 °C. In addition, pH before and after long term immersion tests was measured with a pH meter with temperature compensation function (INESA pH S-3C).

2.2. Electrochemical tests

Electrochemical tests, including polarisation and electrochemical impedance spectroscopy (EIS), were carried out with a Zahner potentiostat (Zennium Pro). The reference electrode was a saturated calomel electrode (all potentials reported with respect to SCE in this work) connected to the solution with a home-made salt bridge filled with agar gel (saturated KCl). The counter electrode was Pt foil (2 cm × 2 cm, 3 mm thick) connected to a polyethylene shank. Stable open circuit potential (OCP) was achieved by immersing the sample in solution for 1 hour, after which anodic/cathodic polarisations (sweep rate 1 mV s^{-1}) were carried out separately to minimise the effect of the opposite reaction, *i.e.* potential sweep started from −20 mV *vs.* OCP to positive direction for anodic polarisation and from +20 mV *vs.* OCP to negative direction for cathodic polarisation. Similarly, EIS tests also required a stable OCP through 1 hour immersion before testing and were performed at the last OCP values measured during immersion. The frequency was from 100 kHz to 10 mHz and the amplitude was 10 mV. EIS data were analysed with Zview software. All electrochemical tests were repeated three times to ensure reproducible results.

2.3. Long term immersion tests

Centrifuge tubes, sterilised and in a V-bottom shape, were used for immersion to minimise the risks of solution pollution and crevice corrosion. The immersed discs had a surface area of 1 cm^2 and were 0.5 cm thick. The total volume of solution was 10 mL, so the volume to surface ratio of immersion tests was 2.65 mL cm^{-2}. Three parallel disc samples were prepared for each kind of solution, immersed separately in three tubes and stored in the incubator (37 °C). In addition, three control samples (containing only solution without any discs) for each kind of solution were also stored together. The tests lasted for 4 months.

After tests, all solutions (liquid phase) were transferred carefully with sterilised syringes to new sterilised tubes and sent for ICP-MS analysis (ELAN DRC-e, PerkinElmer Inc., US) to determine the concentration of released Co, Cr, Mo and Ni in solution. Spectral interference was minimised by the application of DRC. Elemental concentrations of Co, Cr, and Mo for Co−28Cr−6Mo discs and Co, Cr, Mo, and Ni for Co−33Ni−20Cr−10Mo discs were determined. Calibration was based on standard mixed solutions (Reference Materials of China). The limit of detection (LOD) and limit of quantification (LOQ) of the measured elements are provided in ESI.†

The surface oxide film of the discs after immersion tests was analysed by X-ray photoelectron spectroscopy (XPS, Thermo

Scientific Escalab 250Xi) to determine the composition and valence states of metals. Binding energies are relative to Fermi level. Regions of Co2p, Cr2p, and Mo3d were measured for Co−28Cr−6Mo and regions of Co2p, Cr2p, Ni2p, and Mo3d were measured for Co−35Ni−20Cr−10Mo. Survey spectra including C1s and O1s were also recorded for both. The data were analysed with XPS peak software (version 4.1). In addition, a scanning electron microscope (SEM, HITACHI Regulus 8100) and an atomic force microscope (AFM, Bruker MultiMode 8) were applied for surface characterisation after immersion.

3. Results

3.1. Electrochemical tests

Both Co alloys (Co−28Cr−6Mo and Co−35Ni−20Cr−10Mo) were immersed in PS alone (physiological saline), PS with 0.1% albumin and/or 1 mM H_2O_2 for 1 hour to obtain stable OCP and then either anodic or cathodic polarisation was carried out separately for each condition. The results in all electrolytes are shown in Fig. 1.

From Fig. 1a and d, it is seen that the open circuit potentials for both alloys at all conditions became stable within 1 hour (no more than 10 mV change within 5 min). Fig. 1b and e reveal clear anodic passive regions with identical passive current values for both alloys in PS and PS + albumin, while the presented dissolution current near OCP was slightly higher in the presence of albumin (red and green lines). In the presence of H_2O_2, albumin also increased the presented dissolution current value near OCP (blue and black lines). Since H_2O_2 shifted the anodic branch to a much higher potential range, corrosion potential in the presence of H_2O_2 was almost in the passive
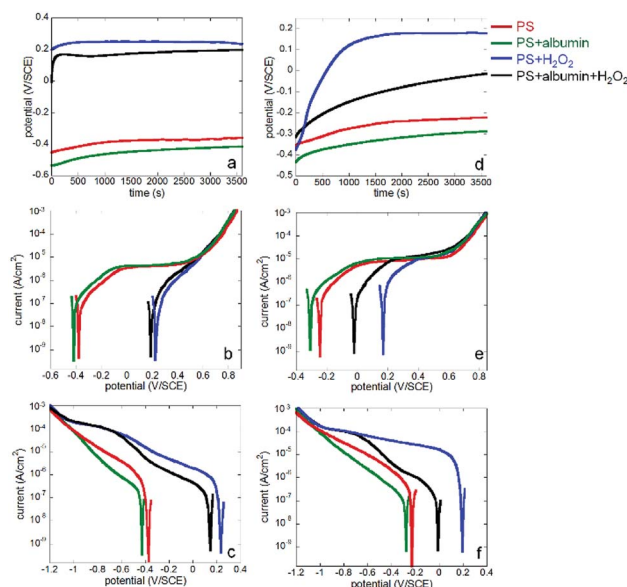

Fig. 1 Electrochemical test results of Co alloys in PS, PS + albumin, PS + H_2O_2 and PS + albumin + H_2O_2 at 37 °C, including 1 h OCP measurements (a and d), anodic polarisation curves (b and d) and cathodic polarisation curves (c and f); a−c are for Co−28Cr−6Mo and d−f are for Co−35Ni−20Cr−10Mo.

potential region in the absence of H_2O_2; anodic currents with and without H_2O_2 cannot be compared.

As for the cathodic curves (Fig. 1c and f), it is clear that the addition of albumin obviously inhibited cathodic reactions when the green and red lines or the blue and black lines are compared, while H_2O_2 largely promoted cathodic reactions when the blue and red lines or the green and black lines are compared.

If Co–28Cr–6Mo and Co–35Ni–20Cr–10Mo alloys are compared, it can be seen that for anodic polarisation tests (Fig. 2), the current densities of Co–35Ni–20Cr–10Mo alloy were consistently higher and both current densities became identical above *ca.* 0.6 V/SCE under all conditions. For cathodic polarisation tests (Fig. 3), cathodic current densities were higher for Co–35Ni–20Cr–10Mo in PS, PS + albumin and PS + H_2O_2 (Fig. 3a–c) and, in the presence of both H_2O_2 and albumin, the cathodic current densities are almost the same for both alloys (Fig. 3d).

Electrochemical impedance spectroscopy measurements were carried out after 1 hour open circuit immersion under all four conditions; Nyquist and Bode plots for both alloys are shown in Fig. 4 (a and b for Co–28Cr–6Mo, c and d for Co–35Ni–10Mo). The applied equivalent circuit is shown in Fig. 5, in which CPE was substituted for capacitance due to the non-homogeneous sample surface. The experiments were repeated three times and Table 3 summarises the fitted values for both alloys. It can be seen that the addition of albumin into PS did not noticeably change the value of R_{ct} (charge transfer resistance) for either alloy, while the addition of H_2O_2 obviously decreased R_{ct} compared to PS. Furthermore, the presence of both H_2O_2 and albumin decreased the R_{ct} values of both alloys by *ca.* 50%, presenting the minimum values. R_f, which is oxide film resistance, basically varied in the same order as R_{ct}. Meanwhile Q_f, which usually provides information on film compactness,[52,53] increased in a reverse manner as R_f, so the compactness of surface oxide was highest in PS but lowest in PS + albumin + H_2O_2; it seems that oxide compactness of PS + albumin was close to PS, while
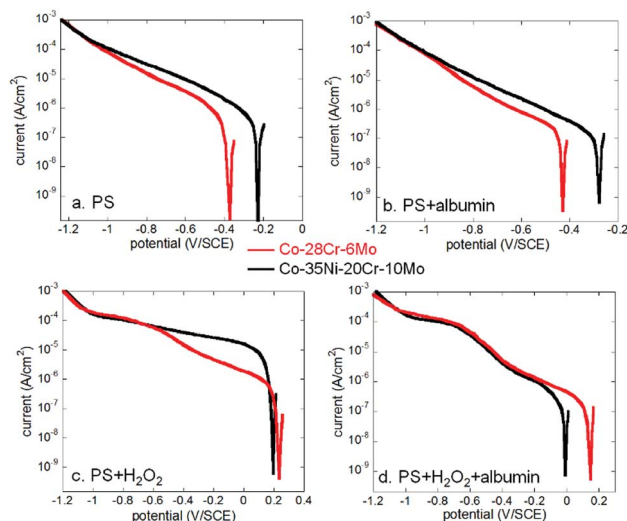

Fig. 3 Comparison of cathodic polarisation curves of Co–28Cr–6Mo and Co–35Ni–20Cr–10Mo in (a) PS, (b) PS + albumin, (c) PS + H_2O_2 and (d) PS + albumin + H_2O_2.

that of PS + H_2O_2 was close to PS + albumin + H_2O_2. In addition, the value of R_s tended to be increased by the addition of H_2O_2 and/or albumin, while the parameters Q_{dl}-n and Q_f-n related to CPE were not largely affected. This parameter indicates the characteristic of a CPE, which is regarded as a pure resistor if $n = 0$ and a pure capacitor if $n = 1$.[52]

3.2. Long term immersion tests

Concentrations of metal release for both alloys measured with ICP-MS after 4 months immersion at 37 °C are compared in Fig. 6. The data corresponding to Fig. 6 are provided in a table in the ESI.† First, it is obvious that the release amount of each metal of Co–35Ni–20Cr–10Mo is larger than those of Co–28Cr–6Mo. Secondly, the addition of only albumin slightly promoted metal release of Co–35Ni–20Cr–10Mo but did not statistically increase that of Co–28Cr–6Mo, while the addition of only H_2O_2 clearly increased metal release of both alloys. Thirdly, in the presence of H_2O_2, albumin clearly increased metal release of both alloys. Lastly, the addition of both species together substantially increased metal release when compared to PS alone, resulting in the largest amount of metal release among the four conditions for both alloys. Nonetheless, Student's *t*-test reveals a synergistic effect of both species only for Co–35Ni–20Cr–10Mo, not for Co–28Cr–6Mo ($p < 0.01$, the amount of metal release in the presence of both species obviously larger than the sum of H_2O_2 alone and albumin alone). The pH was measured before and after this long term immersion test. The pH values of all solutions before and after tests were from 7.1–7.6, so the difference was not found to be remarkable.

In addition to ICP-MS results, XPS measurements were carried out after 4 months immersion. Fig. 7a shows the O1s peak of Co–28Cr–6Mo in PS as an example, which can be deconvoluted into a sub-peak at 530.0 eV (corresponding to lattice oxygen O^{2-}) and a sub-peak at 531.3 eV (corresponding to OH^-).[54] Fig. 7b shows
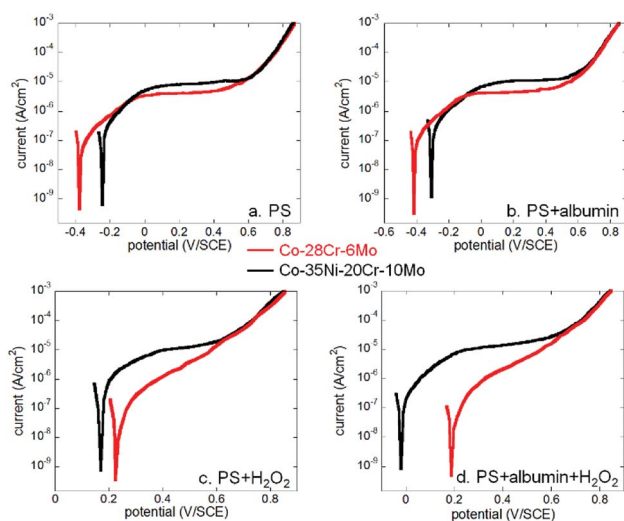

Fig. 2 Comparison of anodic polarisation curves of Co–28Cr–6Mo and Co–35Ni–20Cr–10Mo in (a) PS, (b) PS + albumin, (c) PS + H_2O_2 and (d) PS + albumin + H_2O_2.
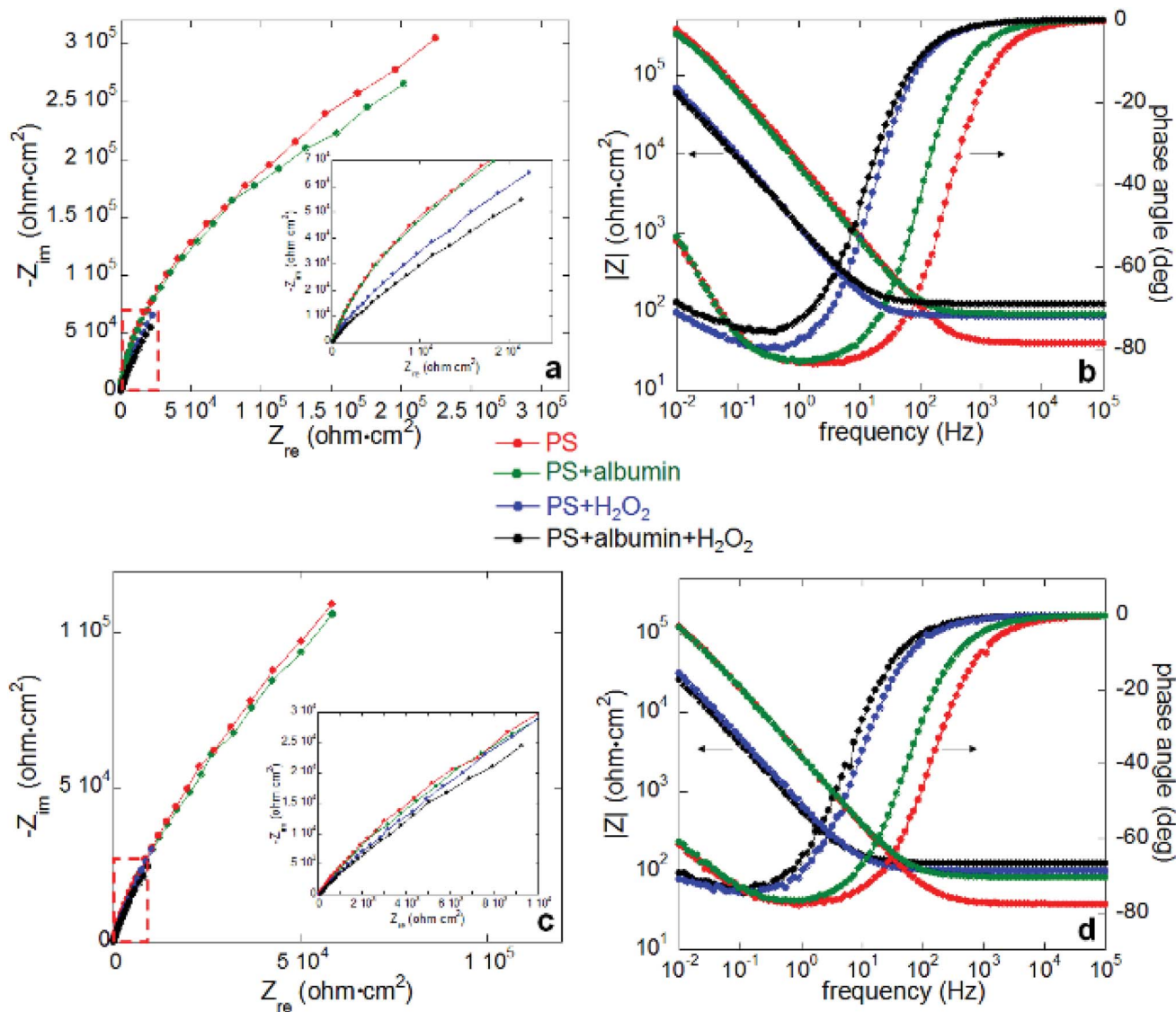
Fig. 4   Nyquist plots and Bode plots of Co−28Cr−6Mo (a and b) and Co−35Ni−20Cr−10Mo (c and d) in PS, PS + albumin, PS + H$_2$O$_2$ and PS + albumin + H$_2$O$_2$ at 37 °C obtained after 1 hour open circuit immersion.
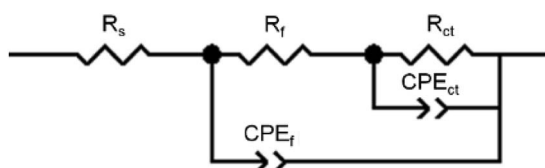

Fig. 5   Equivalent circuit applied to fit the EIS plots in Fig. 4.

a clear peak corresponding to C1s of Co–28Cr–6Mo in PS at 284.6 eV. Similarly, Fig. 7c and d present the O1s and C1s peaks of Co–35Ni–20Cr–10Mo alloy in PS. The related peaks measured for other conditions do not reveal substantial differences, therefore not all O1s and C1s peaks are shown here.

Co2p, Cr2p and Mo3d peaks of both alloys and Ni2p peaks of Co–35Ni–20Cr–10Mo alloy in all four conditions are shown in Fig. 8, 9, 10 and 11, respectively. Generally, it can be observed

that the addition of H$_2$O$_2$ greatly increased the amount of Co, Cr and Mo oxides (Co$_2$O$_3$ 2p$_{3/2}$ at 779.5 eV, Co$_2$O$_3$ 2p$_{1/2}$ at 794.6 eV, CoO 2p$_{3/2}$ at 781.0 eV and CoO 2p$_{1/2}$ at 796.1 eV;[55] Cr$_2$O$_3$ 2p$_{3/2}$ at 576.0 eV, Cr$_2$O$_3$ 2p$_{1/2}$ at 585.8 eV,[24,31,56] CrOOH 2p$_{3/2}$ at 577.0 eV and CrOOH 2p$_{1/2}$ at 587.0 eV;[57] MoO$_2$ 3d$_{3/2}$ at 231.1 eV,[24,31,58] MoO$_3$ 3d$_{5/2}$ at 228.2 eV and MoO$_3$ 3d$_{3/2}$ at 233.5 eV[59]) when compared to PS alone, while albumin decreased the amount of these oxides. It is noticed that hydroxyl oxide was identified for Cr (*i.e.* CrOOH) (Fig. 9), but not for the other metals. As to Ni for Co–35Ni–20Cr–10Mo alloy shown in Fig. 11, a very small shoulder was found near the main peak of Ni^0 2p$_{3/2}$ at 852.7 eV,[31,60,61] indicating a tiny amount of NiO (853.7 eV),[61,62] though the difference between each condition was not sufficiently clear.

To make the differences more visible, the peak areas of each oxide for both alloys in all four conditions are compared in Table 4 and the peak area sums of oxides of Co (Co$_2$O$_3$ and

Table 3 Summarisation of the fitted parameters of EIS plots of Co−28Cr−6Mo and Co−35Ni−20Cr−10Mo alloys in PS, PS + albumin, PS + H_2O_2 and PS + albumin + H_2O_2 at 37 °C after 1 hour open circuit immersion

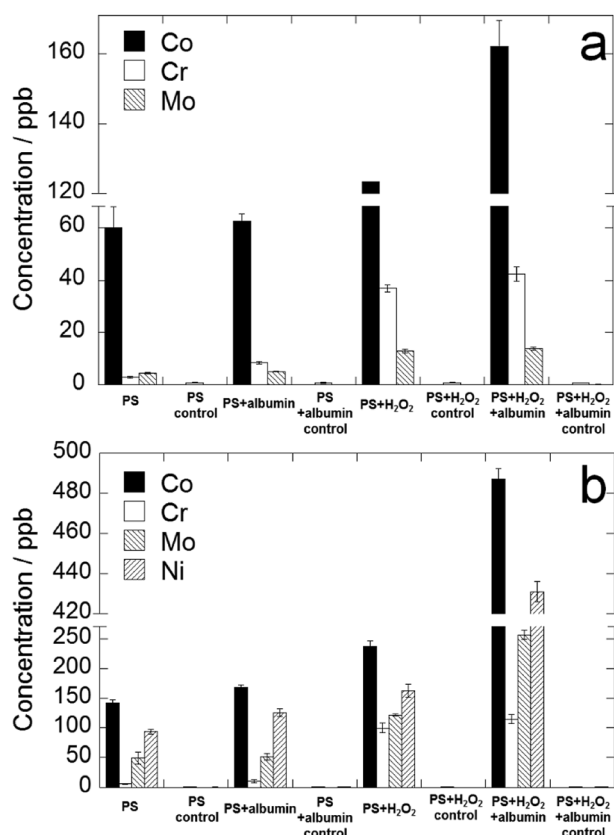|		PS	PS + albumin	PS + H_2O_2	PS + albumin + H_2O_2
Co−28Cr−6Mo	$R_s/\Omega\ cm^2$	38.7 (1.2%)	92.3 (1.0%)	89.7 (1.7%)	124.9 (2.2%)
	$R_{ct}/\Omega\ cm^2$	6.81×10^5 (4.0%)	6.59×10^5 (5.0%)	3.85×10^5 (4.1%)	3.18×10^5 (4.1%)
	$Q_{dl}\text{-}Y/\Omega^{-1}\ cm^{-2}\ s^n$	3.00×10^{-5} (4.5%)	3.75×10^{-5} (3.2%)	4.35×10^{-5} (3.7%)	4.66×10^{-5} (1.9%)
	$Q_{dl}\text{-}n$	0.83 (1.1%)	0.84 (1.9%)	0.84 (1.1%)	0.84 (1.3%)
	$R_f/\Omega\ cm^2$	4.59×10^5 (3.8%)	4.26×10^5 (2.9%)	1.27×10^5 (4.6%)	9.06×10^4 (7.3%)
	$Q_f\text{-}Y/\Omega^{-1}\ cm^{-2}\ s^n$	2.21×10^{-5} (5.2%)	2.46×10^{-5} (3.4%)	1.53×10^{-4} (4.4%)	1.60×10^{-4} (4.0%)
	$Q_f\text{-}n$	0.95 (0%)	0.94 (0%)	0.92 (1.2%)	0.89 (1.3%)
Co−35Ni−20Cr−10Mo	$R_s/\Omega\ cm^2$	37.6 (2.0%)	85.1 (3.3%)	98.8 (1.2%)	122.6 (8.5%)
	$R_{ct}/\Omega\ cm^2$	3.88×10^5 (5.2%)	3.39×10^5 (4.0%)	2.87×10^5 (4.3%)	1.78×10^5 (6.6%)
	$Q_{dl}\text{-}Y/\Omega^{-1}\ cm^{-2}\ s^n$	4.00×10^{-5} (4.2%)	4.40×10^{-5} (2.0%)	5.43×10^{-5} (5.0%)	8.92×10^{-5} (4.2%)
	$Q_{dl}\text{-}n$	0.84 (1.3%)	0.84 (1.9%)	0.83 (1.6%)	0.85 (1.3%)
	$R_f/\Omega\ cm^2$	1.89×10^5 (2.9%)	1.70×10^5 (3.9%)	1.07×10^5 (5.0%)	6.40×10^4 (4.7%)
	$Q_f\text{-}Y/\Omega^{-1}\ cm^{-2}\ s^n$	6.77×10^{-5} (5.6%)	7.06×10^{-5} (5.9%)	2.99×10^{-4} (3.3%)	3.37×10^{-4} (5.1%)
	$Q_f\text{-}n$	0.88 (1.8%)	0.87 (1.0%)	0.87 (1.5%)	0.86 (1.2%)

Fig. 6 Metal release concentrations of (a) Co−28Cr−6Mo and (b) Co−35Ni−20Cr−10Mo after 4 months immersion in PS, PS + albumin, PS + H_2O_2 and PS + albumin + H_2O_2 at 37 °C.

Fig. 7 XPS peaks of (a) O1s and (b) C1s obtained from the surface of Co−28Cr−6Mo alloy in PS and (c) O1S and (d) C1s obtained from the surface of Co−35Ni−20Cr−10Mo alloy in PS after 4 months immersion at 37 °C.

CoO), oxides of Cr (Cr_2O_3 and CrOOH), and oxides of Mo (MoO_2 and MoO_3) are also included. Since arbitrary units are not useful for analysis, the peak area of metallic Co^0,[63] Cr^0,[56,60] Mo^0 (ref. 24 and 31) or Ni^0 (ref. 31, 60, 61, 64 and 65) for each corresponding spectrum is regarded as 1, thus the data presented in Table 4 are actually the ratios 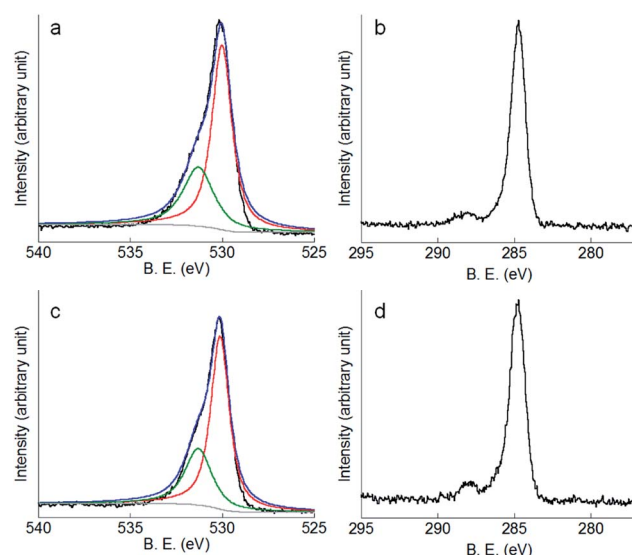of oxides to corresponding metallic components. It is very clear that the presence of albumin and H_2O_2 respectively decreased and increased the amount of oxides, while the coexistence of both species resulted in an in-between amount of oxides. Furthermore, the amount of each surface oxide for Co−35Ni−20Cr−10Mo was consistently larger than that of Co−28Cr−6Mo under all four conditions. The formation of Co oxides was largely promoted by the addition of H_2O_2 for both alloys, while the amounts of Cr and Mo oxides were obviously increased much more for Co−35Ni−20Cr−10Mo than for Co−28Cr−6Mo alloy in the presence of H_2O_2. In addition, the amount of NiO stayed very low for all four conditions and no variation was evident.

Furthermore, AFM was used to compare the surface morphologies of Co−28Cr−6Mo and Co−35Ni−20Cr−10Mo discs
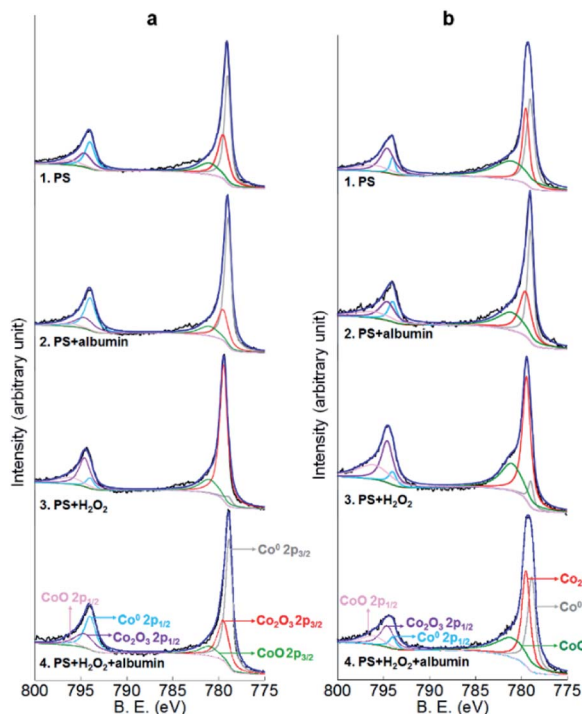
Fig. 8 XPS peaks of Co2p on the surface of (a) Co−28Cr−6Mo and (b) Co−35Ni−20Cr−10Mo after 4 months immersion in PS, PS + albumin, PS + H2O2 and PS + albumin + H_2O_2 at 37 °C.

after immersion (Fig. 12). The difference between PS and PS + albumin was not substantial, while it can be clearly observed that the discs immersed in PS + H_2O_2 presented a different
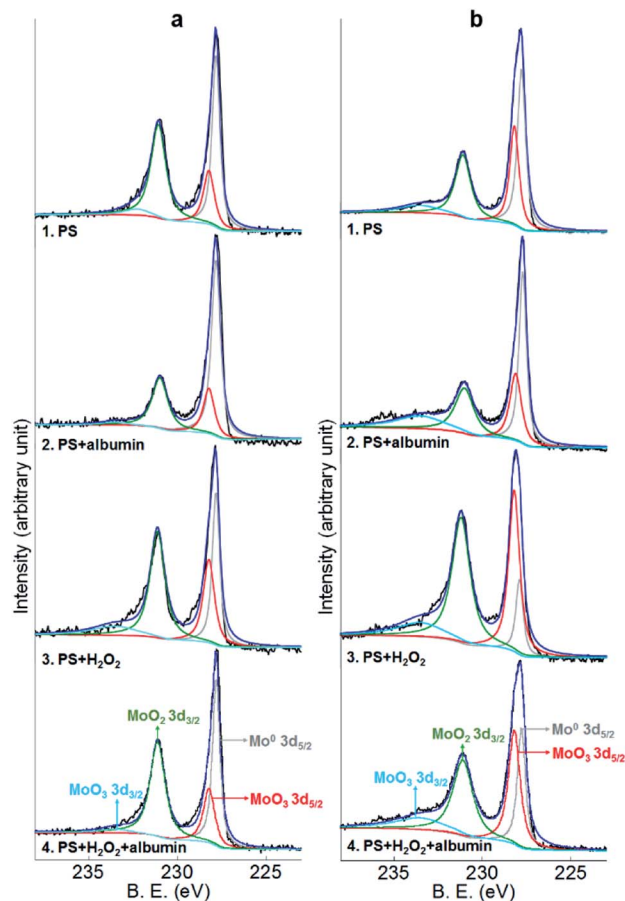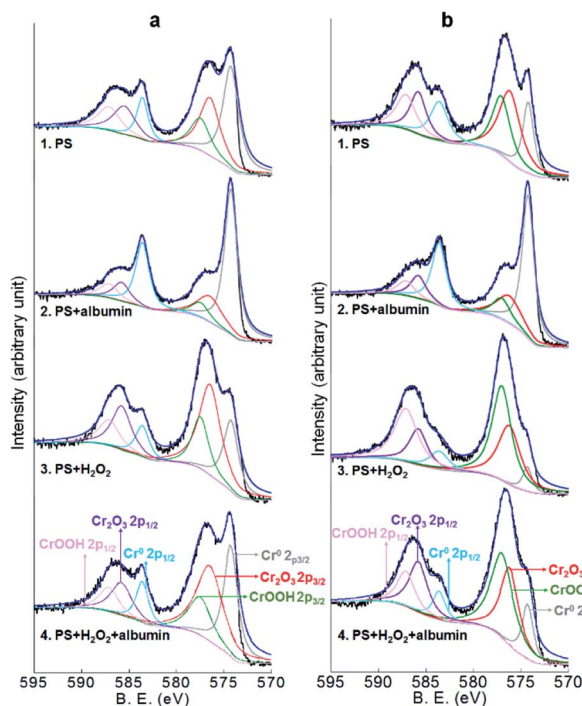

Fig. 10 XPS peaks of Mo3d on the surface of (a) Co−28Cr−6Mo and (b) Co−35Ni−20Cr−10Mo after 4 months immersion in PS, PS + albumin, PS + H_2O_2 and PS + albumin + H_2O_2 at 37 °C.

morphology (Fig. 12c and g) in which the surface was very likely to be covered by a large amount of oxides, concealing some local grinding marks. However, with the addition of albumin (*i.e.* PS + albumin + H_2O_2), grinding marks can be clearly observed again (Fig. 12d and h). In addition, SEM was applied for surface morphology analysis; however, the difference between PS + H_2O_2 and the other conditions was not as clear as that presented by AFM. EDX area scans were also carried out, in which the atomic percentage of element O was shown to be higher than the other conditions, while the difference between PS, PS + albumin and PS + albumin + H_2O_2 was not as clear as the XPS results shown in Fig. 8–10. Therefore, the SEM/EDX results are not shown in this section; instead, they are provided in the ESI.†

4. Discussion

4.1. The effect of albumin

The polarisation curves in Fig. 1 show a slight promotion of anodic reaction and clear depression of cathodic reaction in the presence of albumin. However, the raised anodic current presented near OCP may be due to the suppressed cathodic reaction in the presence of albumin, affecting the anodic branch near the corrosion potential according to mixed potential
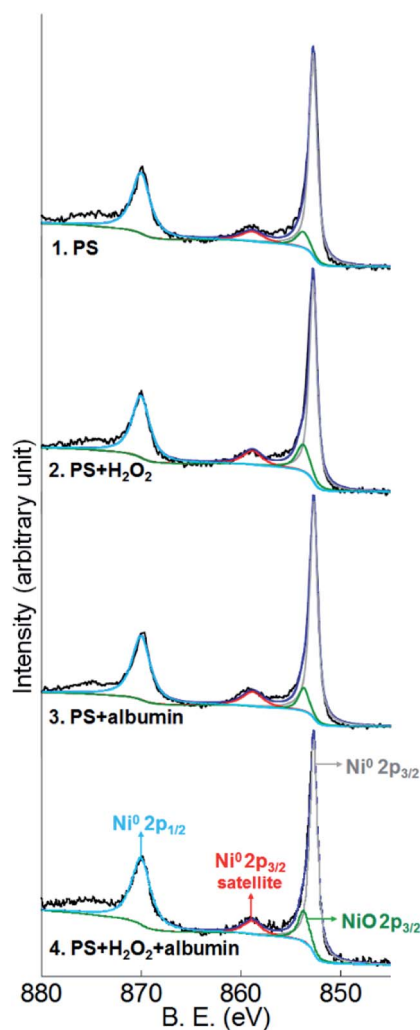

Fig. 9 XPS peaks of Cr2p on the surface of (a) Co−28Cr−6Mo and (b) Co−35Ni−20Cr−10Mo after 4 months immersion in PS, PS + albumin, PS + H_2O_2 and PS + albumin + H_2O_2 at 37 °C.

Fig. 11 XPS peaks of Ni2p on the surface of Co–35Ni–20Cr–10Mo after 4 months immersion in PS, PS + albumin, PS + H_2O_2 and PS + albumin + H_2O_2 at 37 °C.

theory, while the actual anodic dissolution is not necessarily accelerated. According to EIS results, the decrease of R_{ct} due to albumin alone was only determined for Co–35Ni–20Cr–10Mo if errors in Table 3 were considered. The combination of these results with the metal release result (see Section 3.2, *i.e.* the addition of albumin alone increased the metal release of only Co–35Ni–20Cr–10Mo) may imply that albumin alone would not noticeably affect anodic dissolution of Co–28Cr–6Mo and "acceleration of anodic reaction" could only be determined for Co–35Ni–20Cr–10Mo. Accelerated anodic reaction was likely to be ascribed to formation of complexes or chelates between albumin and metals[22,33,66] (spectrophotometric methods proved the tendency for first row transition metal elements, including Co and Cr, to form complexes with proteins),[66] resulting in high reaction rates with metals in substrate and/or surface oxides. However, Hedberg[50] reported decreased amount of Co release in PBS + albumin compared to PBS alone, which was ascribed to precipitation of Co–BSA complexes, not detectable by ASS technique, though the constituents and concentrations of solutions were different and the immersion time was shorter than this study.

As to the cathodic reaction, the inhibitive effect can likely be ascribed to adsorption of albumin on the metal surface, blocking the effective areas for reduction reactions[67] or suppressing the access of oxidant.[68] Albumin acting as a cathodic inhibitor has also been reported on Ti alloys[8] and stainless steel 316L.[11]

According to the Evans diagram, the anodic current increase and cathodic current decrease should both result in a negative shift of corrosion potential; the more the anodic increasing or cathodic decreasing effect of albumin, the more the negative shift of corrosion potential. However, since the negative shifts compared to PS alone were all very small (Fig. 1), the influence on anodic or cathodic reaction as stated in the above paragraph is not believed to be substantial. This agrees with the EIS results revealing that albumin exerted a slight effect on the value of R_{ct} compared to PS alone (Table 3). The reduction of the amount of

Table 4 Comparison of amount of each oxide on the surface of Co–28Cr–6Mo and Co–35Ni–20Cr–10Mo after 4 months immersion in PS, PS + albumin, PS + H_2O_2 and PS + albumin + H_2O_2 at 37 °C; the comparison is based on the peak area data obtained from XPS measurements and normalisation was applied by setting the peak area of metallic Co^0, Cr^0, Mo^0 or Ni^0 as 1 for each corresponding spectrum

|		CoO	Co_2O_3	Cr_2O_3	CrOOH	MoO_2	MoO_3	NiO
Co–28Cr–6Mo	PS	0.32	0.67	0.87	0.56	1.12	0.58	—
		Sum: 0.99		Sum: 1.43		Sum: 1.70		—
	PS + albumin	0.24	0.44	0.36	0.20	0.51	0.37	—
		Sum: 0.68		Sum: 0.56		Sum: 0.88		—
	PS + H_2O_2	2.77	8.93	1.86	0.93	1.41	1.21	—
		Sum: 11.70		Sum: 2.79		Sum: 2.62		—
	PS + albumin + H_2O_2	0.22	0.69	1.29	0.65	1.06	0.58	—
		Sum: 0.91		Sum: 1.94		Sum: 1.64		—
Co–35Ni–20Cr–10Mo	PS	1.12	1.12	1.49	1.20	0.77	0.95	0.15
		Sum: 2.24		Sum: 2.69		Sum: 1.72		—
	PS + albumin	0.87	0.99	0.41	0.25	0.59	1.03	0.11
		Sum: 1.86		Sum: 0.66		Sum: 1.62		—
	PS + H_2O_2	5.34	6.39	3.38	5.25	4.04	4.32	0.15
		Sum: 11.73		Sum: 8.63		Sum: 8.36		—
	PS + albumin + H_2O_2	1.00	1.30	2.40	2.55	1.55	2.00	0.13
		Sum: 2.30		Sum: 4.95		Sum: 3.55		—
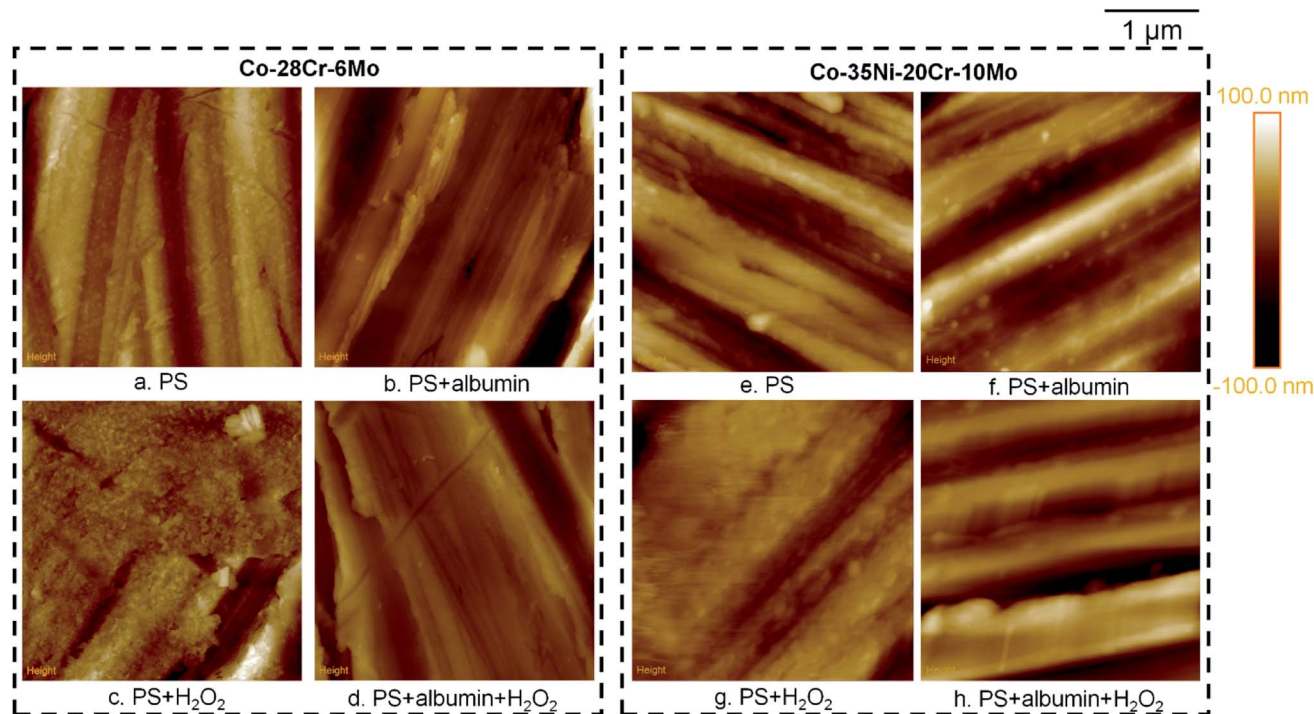
Fig. 12 AFM images of the surface of Co−28Cr−6Mo discs in (a) PS, (b) PS + albumin, (c) PS + H_2O_2 and (d) PS + albumin + H_2O_2 and Co−35Ni−20Cr−10Mo in (e) PS, (f) PS + albumin, (g) PS + H_2O_2 and (h) PS + albumin + H_2O_2 after 4 months immersion at 37 °C.

surface oxides by albumin indicates that it may facilitate the dissolution of oxides (Table 4), which can be related to the slightly decreased R_f (Table 3) and slightly increased metal release (Fig. 6).

4.2. The effect of H_2O_2

The addition of H_2O_2 largely promoted the cathodic reaction rates (Fig. 1) because H_2O_2 can be reduced with dissolved oxygen, contributing to cathodic current and raising corrosion potential. The effect of H_2O_2 on anodic reactions cannot be characterised by polarisation curves since the increase of corrosion potential moved the anodic branch to a relatively high potential range and a large cathodic current may conceal the actual anodic information near corrosion potential, so even the passive region could not be fully observed. However, electrochemical impedance spectroscopy reveals a clear decrease of R_{ct} by H_2O_2 (Table 3), which can be well correlated to the largely increased amount of metal release (Fig. 6). H_2O_2 acting as a dissolution accelerator for Co alloys has also been reported previously.[12] In terms of H_2O_2, the anodic current increase and cathodic current increase should tend to move the corrosion potential in the negative and positive directions, respectively. The cathodic current increase prevailed under the circumstances in this study, resulting in the observed positive shift of corrosion potential for both alloys (Fig. 1).

Furthermore, according to XPS results, the amount of each kind of surface oxide was drastically increased by H_2O_2, which is a strong oxidant (the atomic percentage of O was also found to be raised by the presence of H_2O_2 according to EDX results provided in ESI†), especially for the oxides on Co−35Ni−20Cr−

10Mo alloy and for Co oxides on both alloys (Table 4). This can be supported by the AFM images shown in Fig. 12c and g. Since X-rays penetrate into oxide film and may detect the metal substrate, stronger oxide peaks and weaker metal substrate peaks indicate thicker oxide films. Although the formation of surface oxides should lead to thickening of the oxide film, it did not provide effective corrosion barriers, but instead made the film less corrosion resistant (both R_{ct} and R_f were greatly decreased). It is suggested that the oxides formed due to the presence of H_2O_2 cannot maintain a compact passive film, resulting in a lack of corrosion resistance. Since less compact film may allow more interior electrolyte, the loss of compactness due to H_2O_2 can also be supported by the decrease of R_f and increase of Q_f. In addition, hydroxyl oxide was found for Cr (i.e. CrOOH), and its formation was largely promoted by H_2O_2 through the Fenton reaction, which was also reported on CoCrMo alloy[45] and stainless steel 316L;[11] however, the increase of the amount of CrOOH in passive film is not likely to provide an effective corrosion barrier either.

4.3. The effect of coexistence of albumin and H_2O_2

As stated in Section 4.1, an addition of albumin alone only slightly promoted the anodic dissolution of Co−35Ni−20Cr−10Mo, but not statistically for Co−28Cr−6Mo, so it may be suggested that Co alloys are not sensitive to albumin alone. However, the promoting effect of albumin was much more obvious in the presence of H_2O_2 for both Co alloys, demonstrated by both EIS and metal release data. This is not the same for Ti alloys[8] or stainless steel 316L.[11] The former presented

a decrease of anodic dissolution while the latter showed obvious increase of anodic dissolution in the presence of albumin alone.

Although H_2O_2 drastically facilitated increase of the amount of oxides, albumin favoured the dissolution of surface oxides formed due to H_2O_2 (or inhibited the formation of oxides due to H_2O_2), making the amount of oxide fall to near the level of PS alone, but without elimination of any oxides or introduction of new ones. However, according to EIS and metal release results (Table 3 and Fig. 6), corrosion resistance of either alloy was largely lowered by the presence of both species when compared to PS alone. Therefore, it is suggested that the surface oxides in the presence of both species should exhibit much lower compactness than PS alone.

Given the similar level of oxide amounts in PS alone and PS + albumin + H_2O_2, it seems that the tendency of oxide formation due to H_2O_2 and the tendency of oxide dissolution due to albumin were balanced to some extent, but the suggested low compactness in the presence of both species indicates that the effect of H_2O_2 actually prevailed in deciding the corrosion protection characteristics of passive film, although the effect of H_2O_2 facilitating oxide formation was suppressed by albumin. Considering the very slight change of R_{ct}, R_f and Q_f values (Table 3) induced by albumin, it is not believed to induce essential change in film compactness; instead, its presence only thinned the oxide film to slightly decrease corrosion resistance. It can also be speculated from the Q_f values that the compactness of PS + H_2O_2 and PS + albumin + H_2O_2 may be on similar levels and those of PS and PS + albumin should be on another relatively higher level.

It has also been noticed that the decreased amount of oxides due to albumin was much higher in the presence of H_2O_2 than in the absence of H_2O_2 (Table 4), because the negatively charged carboxylate groups of albumin, which are believed to be a key component for complexing with metals,[22,31] may permeate/enter into less compact film more easily to interact with the oxides of larger amount, leading to even lower compactness. In addition, the H_2O_2-induced oxides tended to leach out in the presence of albumin, inducing more metal release into bulk solution.

The above discussion suggests that corrosion behaviours of Co alloys in this environment should be mainly decided by the characteristics of the oxides, including film compactness and thickness. However, mixed potential theory, which interpreted the corrosion mechanism of Ti alloy,[8] is not suitable for Co alloys. In addition, it is worth mentioning that although H_2O_2 may react with albumin during the incubation period, reducing the concentration of H_2O_2 and/or albumin which is likely to have led to an under-estimation of the amount of released metal compared with that expected if this had been controlled for, the interpretation of the data shown in this work is not affected, *i.e.* a remarkable effect in terms of metal release was still observed and ascribed to the co-existence of both species, compared to PS alone and PS with either species. Therefore, H_2O_2 would not be completely consumed by albumin in this study and *vice versa*.

4.4. Between Co–28Cr–6Mo and Co–35Ni–20Cr–10Mo

It is observed from polarisation curves that anodic and cathodic currents in the presence of both species were respectively higher

and lower than in PS + H_2O_2, which agrees with the comparison between PS + albumin and PS alone (Fig. 1), so the effect of albumin is consistent regardless of the existence of H_2O_2. However, it is noticed that the increased range of anodic current for Co–35Ni–20Cr–10Mo alloy in the presence of both species when compared to PS + H_2O_2 was larger than Co–28Cr–6Mo alloy, which agrees with the decrease range of R_{ct} (*i.e.* decreased by *ca.* 17.4% for Co–28Cr–6Mo and *ca.* 38.0% for Co–35Ni–20Cr–10Mo, Table 3) and the increase range of metal release (*i.e.* increased by *ca.* 25.9% for Co–28Cr–6Mo and *ca.* 107.6% for Co–35Ni–20Cr–10Mo as calculated from ESI†) under open circuit conditions. In addition, the increase range of metal release between PS + albumin + H_2O_2 and PS + albumin was also bigger for Co–35Ni–20Cr–10Mo. Therefore, the influence of the coexistence of both species was more remarkable for Co–35Ni–20Cr–10Mo (compared to either species alone), agreeing with the fact that synergistic effect was observed for Co–35Ni–20Cr–10Mo. It is very clear that Co–28Cr–6Mo is more reliable than Co–35Ni–20Cr–10Mo in the presence of albumin and H_2O_2. It was also noticed that metal release of Co–28Cr–6Mo was more than 316L[11] in PS alone, but much less severe than stainless steel 316L[11] in the presence of albumin and H_2O_2 (although the test for stainless steel 316L used less concentrated H_2O_2), implying relatively higher reliability of Co–28Cr–6Mo than stainless steel 316L with the effect of both species.

It is also observed that all current densities became identical and increased drastically from *ca.* 0.6 V/SCE for both alloys (Fig. 1), which should be ascribed to the anodic dissolution of Cr_2O_3 to $Cr_2O_7^{2-}$ and/or CrO_4^{2-} and is not likely to be related to oxide dissolution of the other metals based on corresponding Pourbaix diagrams.[69] Since H_2O_2 can shift corrosion potential positively, it is possible that a sufficiently high concentration of H_2O_2 may lead to dissolution of Cr_2O_3 and cause serious damage. However, this was not observed in this work for the range of ~1 mM.

As to the cathodic branch, the decrease range of cathodic current in the presence of both species when compared to PS + H_2O_2 was larger for Co–35Ni–20Cr–10Mo than Co–28Cr–6Mo. Since the decrease range of cathodic current in PS + albumin compared with PS alone did not show a noticeable difference between the two alloys (O_2 reduction mainly contributing to cathodic current for these circumstances), this difference is believed to be ascribed to a different reduction rate of H_2O_2, with albumin possibly exerting a more inhibitive effect on the cathodic reduction of H_2O_2 on the surface of Co–35Ni–20Cr–10Mo than Co–28Cr–6Mo.

Generally, from the polarisation curves shown in Fig. 2, the anodic branch is consistently higher for Co–35Ni–20Cr–10Mo at each condition, confirmed by metal release and EIS results obtained at open circuit. According to Table 4, the compositions of oxide films under each condition did not differ substantially between alloys, except for trace NiO for Co–35Ni–20Cr–10Mo, which is not likely to play a significant role in corrosion resistance (it has been reported that the stability of Ni oxides is low,[70] so they would appear scarcely in oxide films), so the difference in corrosion resistance between both alloys may be ascribed to the compactness instead of the constituents of the passive film.

This is also supported by consistently higher Q_f values for Co–35Ni–20Cr–10Mo under each condition. With the expected hazardous Co and Cr release, the synergistic effect of albumin and H_2O_2 on Co–35Ni–20Cr–10Mo also induced a large amount of Ni release, obviously higher than PS alone and PS with solely albumin or H_2O_2, which cannot be overlooked due to its toxicity,[71] causing skin allergies, liver damage, *etc.*; hence, the application of Co–35Ni–20Cr–10Mo in the human body is suggested to be decreased.

Corrosion of both alloys was largely promoted by albumin and H_2O_2, implying an evident insufficiency of standardised methods for corrosion resistance evaluation in biomedical alloys using physiological saline[72,73] and suggesting that more realistic conditions have to be considered.

5. Conclusions

The effects of albumin and/or H_2O_2 on corrosion of biomedical Co alloys (Co–28Cr–6Mo and Co–35Ni–20Cr–10Mo) were investigated in this study *via* electrochemical and long term immersion tests and the coexistence of both species was explored for the first time. Electrochemical tests and long term immersion tests must be combined to draw reliable conclusions.

Co alloy dissolution was not very sensitive to the addition of albumin alone, which slightly increased metal release of Co–35Ni–20Cr–10Mo and did not noticeably affect Co–28Cr–6Mo, while albumin thinned surface oxide films (*i.e.* facilitating dissolution of oxides) of both alloys. The presence of H_2O_2 largely promoted anodic dissolution and metal release, but simultaneously thickened surface oxide film (*i.e.* facilitating formation of oxide film) without changing the basic composition of oxides, implying a decrease in the compactness of passive film.

The coexistence of albumin and H_2O_2 resulted in the largest amount of metal release and lowest corrosion resistance for both Co alloys, which is ascribed to lowered compactness of the passive film, considering the similar composition and amount of surface oxides as in physiological saline. Therefore, the promotion of corrosion by the presence of both species is due to the combined effects of H_2O_2 lowering the compactness of the passive film and albumin facilitating the dissolution/thinning of surface oxides.

The corrosion resistance of Co–28Cr–6Mo is consistently higher than Co–35Ni–20Cr–10Mo based on all techniques applied in this study. Although the coexistence of albumin and H_2O_2 clearly results in the highest corrosion rate for either alloy, a synergistic effect was only demonstrated for Co–35Ni–20Cr–10Mo. In addition, the complexity of the human body environment cannot be neglected for evaluation of the reliability of biomedical alloys applied in the human body and standard tests using physiological saline alone for corrosion resistance evaluation are absolutely insufficient.

Conflicts of interest

There are no conflicts to declare.

Acknowledgements

References

1 S. Pramanik, A. K. Agarwal and K. N. Rai, *Trends Biomater. Artif. Organs*, 2005, **19**, 15–26.

2 Y. P. Liu and J. L. Gilbert, *Electrochim. Acta*, 2018, **262**, 252–263.

3 Y. Okazaki and E. Gotoh, *Biomaterials*, 2005, **26**, 11–21.

4 P. Panigrahi, Y. F. Liao, M. T. Mathew, A. Fischer, M. A. Wimmer, J. J. Jacobs and L. D. Marks, *J. Biomed. Mater. Res., Part B*, 2014, **102**, 850–859.

5 S. Virtanen, I. Milosev, E. Gomez-Barrena, R. Trebse, J. Salo and Y. T. Konttinen, *Acta Biomater.*, 2008, **4**, 468–476.

6 Z. J. Xu, H. F. Lu, J. Lu, C. Lv, X. B. Zhao and G. C. Wang, *RSC Adv.*, 2018, **8**, 3051–3060.

7 M. Talha, C. K. Behera, S. Kumar, O. Pal, G. Singh and O. P. Sinha, *RSC Adv.*, 2014, **4**, 13340–13349.

8 F. Yu, O. Addison and A. J. Davenport, *Acta Biomater.*, 2015, **26**, 355–365.

9 J. L. Wang, R. L. Liu, T. Majumdar, S. A. Mantri, V. A. Ravi, R. Banerjee and N. Birbilis, *Acta Biomater.*, 2017, **54**, 469–478.

10 Y. Zhang, O. Addison, P. F. Gostin, A. Morrell, A. J. M. C. Cook, A. Liens, J. Wu, K. Ignatyev, M. Stoica and A. Davenport, *J. Electrochem. Soc.*, 2017, **164**, C1003–C1012.

11 W. Xu, F. Yu, L. Yang, B. Zhang, B. Hou and Y. Li, *Mater. Sci. Eng., C*, 2018, **92**, 11–19.

12 Y. P. Liu, PhD thesis, The effects of simulated inflammatory conditions on the corrosion and fretting corrosion of CoCrMo alloy, Syracuse University, Syracuse, NY, US, 2017.

13 C. N. Younkin, *J. Biomed. Mater. Res.*, 1974, **8**, 219–226.

14 G. P. Ussia, V. Cammalleri, M. Mule, M. Scarabelli, M. Barbanti, F. Scardaci, S. Mangiafico, S. Imme, D. Capodanno and C. Tamburino, *Catheter. Cardiovasc. Interv.*, 2009, **74**, 607–614.

15 M. Prasad, M. W. Reiterer and K. S. Kumar, *Mater. Sci. Eng., A*, 2014, **610**, 326–337.

16 M. A. Mezour, Y. Oweis, A. A. El-Hadad, S. Algizani, F. Tamimi and M. Cerruti, *RSC Adv.*, 2018, **8**, 23191–23198.

17 M. Haeri and J. L. Gilbert, *Acta Biomater.*, 2013, **9**, 9220–9228.

18 A. W. E. Hodgson, S. Kurz, S. Virtanen, V. Fervel, C. O. A. Olsson and S. Mischler, *Electrochim. Acta*, 2004, **49**, 2167–2178.

19 J. J. Jacobs, A. K. Skipor, P. F. Doorn, P. Campbell, T. P. Schmalzried, J. Black and H. C. Amstutz, *Clin. Orthop. Relat. Res.*, 1996, S256–S263.

20 Z. J. Guo, X. L. Pang, Y. Yan, K. W. Gao, A. A. Volinsky and T. Y. Zhang, *Appl. Surf. Sci.*, 2015, **347**, 23–34.

21 M. L. Rudee and T. M. Price, *J. Biomed. Mater. Res.*, 1985, **19**, 57–66.

22 S. Omanovic and S. G. Roscoe, *Langmuir*, 1999, **15**, 8315–8321.

23 S. Hohn, S. Virtanen and A. R. Boccaccini, *Appl. Surf. Sci.*, 2019, **464**, 212–219.

24 S. Karimi, T. Nickchi and A. M. Alfantazi, *Appl. Surf. Sci.*, 2012, **258**, 6087–6096.

25 C. V. Vidal, A. O. Juan and A. L. Munoz, *Colloids Surf., B*, 2010, **80**, 1–11.

26 H. H. Huang, *Biomaterials*, 2003, **24**, 275–282.

27 W. Wang, F. Mohammadi and A. Alfantazi, *Corros. Sci.*, 2012, **57**, 11–21.

28 M. Afonso, R. Jaimes, E. P. G. Areas, M. R. Capri, E. Oliveira and S. M. L. Agostinho, *Colloids Surf., A*, 2008, **317**, 760–763.

29 S. Karimi, T. Nickchi and A. Alfantazi, *Corros. Sci.*, 2011, **53**, 3262–3272.

30 J. L. Woodman, J. Black and S. A. Jiminez, *J. Biomed. Mater. Res.*, 1984, **18**, 99–114.

31 S. Karimi and A. M. Alfantazi, *Mater. Sci. Eng., C*, 2014, **40**, 435–444.

32 A. C. Lewis, M. R. Kilburn, I. Papageorgiou, G. C. Allen and C. P. Case, *J. Biomed. Mater. Res., Part A*, 2005, **73A**, 456–467.

33 K. Merritt and S. A. Brown, *J. Biomed. Mater. Res.*, 1988, **22**, 111–120.

34 S. Karimi and A. M. Alfantazi, *J. Electrochem. Soc.*, 2013, **160**, C206–C214.

35 J. L. Gilbert, S. Sivan, Y. P. Liu, S. B. Kocagoz, C. M. Arnholt and S. M. Kurtz, *J. Biomed. Mater. Res., Part A*, 2015, **103**, 211–223.

36 J. M. Anderson, A. Rodriguez and D. T. Chang, *Semin. Immunol.*, 2008, **20**, 86–100.

37 D. L. Laskin and K. J. Pendino, *Annu. Rev. Pharmacol. Toxicol.*, 1995, **35**, 655–677.

38 G. M. Rosen, S. Pou, C. L. Ramos, M. S. Cohen and B. E. Britigan, *FASEB J.*, 1995, **9**, 200–209.

39 D. Cadosch, E. Chan, O. P. Gautschi, H. P. Simmen and L. Filgueira, *J. Orthop. Res.*, 2009, **27**, 841–846.

40 H. Y. Lin and J. D. Bumgardner, *Biomaterials*, 2004, **25**, 1233–1238.

41 S. T. Test and S. J. Weiss, *J. Biol. Chem.*, 1984, **259**, 399–405.

42 C. S. Ryan and I. Kleinberg, *Arch. Oral Biol.*, 1995, **40**, 753–763.

43 J. Pan, D. Thierry and C. Leygraf, *J. Biomed. Mater. Res.*, 1996, **30**, 393–402.

44 A. I. Munoz, J. Schwiesau, B. M. Jolles and S. Mischler, *Acta Biomater.*, 2015, **21**, 228–236.

45 Y. P. Liu and J. L. Gilbert, *J. Biomed. Mater. Res., Part B*, 2018, **106**, 209–220.

46 E. K. Brooks, R. P. Brooks and M. T. Ehrensberger, *Mater. Sci. Eng., C*, 2017, **71**, 200–205.

47 C. J. Morris, J. R. Earl, C. W. Trenam and D. R. Blake, *Int. J. Biochem. Cell Biol.*, 1995, **27**, 109–122.

48 J. Prousek, *Pure Appl. Chem.*, 2007, **79**, 2325–2338.

49 S. J. Stohs and D. Bagchi, *Free Radical Biol. Med.*, 1995, **18**, 321–336.

50 Y. Hedberg and I. O. Wallinder, *J. Biomed. Mater. Res., Part B*, 2014, **102**, 693–699.

51 C. Trépanier, R. Venugopalan, R. Messer, J. Zimmerman and A. R. Pelton, *Effect of passivation treatments on nickel release from nitinol, 6th World Biomaterials Congress*, Society for Biomaterials, Mount Laurel, NJ, 2000, pp. 1043.

52 Q. Guo, K. Du, X. Zhu, R. Wang, Y. Xu and F. Wang, *Corros. Sci. Prot. Technol.*, 2013, **25**, 89–94.

53 Q. Guo, K. Du, X. Zhu, Y. Xu, R. Wang and F. Wang, *Electroplat. Pollut. Control*, 2013, **33**, 29–32.

54 S. Ponce, M. A. Peña and J. L. G. Fierro, *Appl. Catal., B*, 2000, **24**, 193–205.

55 B. F. Jin, X. D. Wu, D. Weng, S. Liu, T. T. Yu, Z. Zhao and Y. C. Wei, *J. Colloid Interface Sci.*, 2018, **532**, 579–587.

56 A. Fonseca-Garcia, J. Perez-Alvarez, C. C. Barrera, J. C. Medina, A. Almaguer-Flores, R. B. Sanchez and S. E. Rodil, *Mater. Sci. Eng., C*, 2016, **66**, 119–129.

57 L. Y. Zhao, A. C. Siu, L. J. Pariag, Z. H. He and K. T. Leung, *J. Phys. Chem. C*, 2007, **111**, 14621–14624.

58 H. Luo, H. Z. Su, C. F. Dong and X. G. Li, *Appl. Surf. Sci.*, 2017, **400**, 38–48.

59 A. Koos, A. Oszko and F. Solymosi, *Appl. Surf. Sci.*, 2007, **253**, 3022–3028.

60 J. M. Bastidas, C. L. Torres, E. Cano and J. L. Polo, *Corros. Sci.*, 2002, **44**, 625–633.

61 A. P. Grosvenor, M. C. Biesinger, R. S. Smart and N. S. McIntyre, *Surf. Sci.*, 2006, **600**, 1771–1779.

62 Q. Liu, L. F. Wei, S. Yuan, X. Ren, Y. Zhao, Z. Y. Wang, M. H. Zhang, L. Y. Shi and D. D. Li, *J. Mater. Sci.*, 2015, **50**, 6668–6676.

63 H. Y. Zhao, J. X. Hao, Y. P. Ban, Y. F. Sha, H. C. Zhou and Q. S. Liu, *Catal. Today*, 2019, **319**, 145–154.

64 S. Zafeiratos and S. Kennou, *Surf. Sci.*, 2001, **482**, 266–271.

65 J. J. Jiang, H. Wang, H. H. Guo, T. Yang, W. S. Tang, D. Li, S. Ma, D. Y. Geng, W. Liu and Z. D. Zhang, *Nanoscale Res. Lett.*, 2012, **7**, 1–7.

66 G. C. F. Clark and D. F. Williams, *J. Biomed. Mater. Res.*, 1982, **16**, 125–134.

67 Y. C. Tang, S. Katsuma, S. Fujimoto and S. Hiromoto, *Acta Biomater.*, 2006, **2**, 709–715.

68 X. L. Cheng and S. G. Roscoe, *Biomaterials*, 2005, **26**, 7350–7356.

69 M. Pourbaix, *Atlas of electrochemical equilibria in aqueous solutions*, National Association of Corrosion Engineers, Houston, 2nd edn, 1974.

70 R. Kirchheim, B. Heine, H. Fischmeister, S. Hofmann, H. Knote and U. Stolz, *Corros. Sci.*, 1989, **29**, 899–917.

71 T. H. Li, P. C. Wong, S. F. Chang, P. H. Tsai, J. S. C. Jang and J. C. Huang, *Mater. Sci. Eng., C*, 2017, **75**, 1–6.

72 ASTM F1801-97, *Standard practice for corrosion fatigue testing of metallic implant materials*, ASTM International, West Conshohocken, PA, 2014, http://www.astm.org.

73 ASTM F1875-98, *Standard practice for fretting corrosion testing of modular implant interfaces: Hip femoral head-bore and cone taper interface*, ASTM International, West Conshohocken, United States, 2014, http://www.astm.org.